

## Deterministic Entanglement Swapping in a Superconducting Circuit

Wen Ning,<sup>1</sup> Xin-Jie Huang,<sup>1</sup> Pei-Rong Han,<sup>1</sup> Hekang Li,<sup>2</sup> Hui Deng,<sup>4,5</sup> Zhen-Biao Yang,<sup>1,\*</sup> Zhi-Rong Zhong,<sup>1</sup>  
Yan Xia,<sup>1</sup> Kai Xu,<sup>2,3,†</sup> Dongning Zheng,<sup>2,3</sup> and Shi-Biao Zheng<sup>1,‡</sup>

<sup>1</sup>*Fujian Key Laboratory of Quantum Information and Quantum Optics, College of Physics and Information Engineering, Fuzhou University, Fuzhou, Fujian 350108, China*

<sup>2</sup>*Institute of Physics and Beijing National Laboratory for Condensed Matter Physics, Chinese Academy of Sciences, Beijing 100190, China*

<sup>3</sup>*CAS Center for Excellence in Topological Quantum Computation, University of Chinese Academy of Sciences, Beijing 100190, China*

<sup>4</sup>*Hefei National Laboratory for Physical Sciences at Microscale and Department of Modern Physics, University of Science and Technology of China, Hefei, Anhui 230026, China*

<sup>5</sup>*CAS Centre for Excellence and Synergetic Innovation Centre in Quantum Information and Quantum Physics, University of Science and Technology of China, Hefei, Anhui 230026, China*

 (Received 18 March 2019; published 9 August 2019)

Entanglement swapping, the process to entangle two particles without coupling them in any way, is one of the most striking manifestations of the quantum-mechanical nonlocal characteristic. Besides fundamental interest, this process has applications in complex entanglement manipulation and quantum communication. Here we report a high-fidelity, unconditional entanglement swapping experiment in a superconducting circuit. The measured concurrence characterizing the qubit-qubit entanglement produced by swapping is above 0.75, confirming most of the entanglement of one qubit with its partner is deterministically transferred to another qubit that has never interacted with it. We further realize delayed-choice entanglement swapping, showing whether two qubits previously behaved as in an entangled state or as in a separable state is determined by a later choice of the type of measurement on their partners. This is the first demonstration of entanglement-separability duality in a deterministic way.

DOI: 10.1103/PhysRevLett.123.060502

Quantum entanglement, lying at the heart of the Einstein-Podolsky-Rosen (EPR) paradox [1], is one of the most striking features of quantum mechanics. When two particles are put in an entangled state, they can exhibit nonlocal correlation that cannot be interpreted in terms of any classical model as evidenced by violation of Bell's inequalities [2,3]. In addition to fundamental tests of quantum mechanics, entanglement is an essential resource for many quantum information tasks, such as quantum teleportation [4] and measurement-based quantum computation [5]. The nonlocal characteristic of quantum-mechanical wave functions allows two particles that have never interacted to be put into an entangled state by means of entanglement swapping [6]. The process is illustrated in Fig. 1, where the two qubits ( $Q_1$  and  $Q_4$ ) to be entangled are first entangled with their respective partners ( $Q_2$  and  $Q_3$ ):  $Q_1$  and  $Q_2$  form the first entangled Bell pair, while  $Q_3$  and  $Q_4$  form the second pair. Then a joint Bell state measurement applied to the partners  $Q_2$  and  $Q_3$  will project the remaining two qubits,  $Q_1$  and  $Q_4$ , to one of four possible Bell states; which entangled state is produced depends on the outcome of the Bell state measurement. Aside from fundamental interest, entanglement swapping has practical applications in quantum communication [7] and in multipartite entanglement manipulation necessary for construction of complex quantum networks [8].

Entanglement swapping has been experimentally demonstrated with photonic qubits [9–17]. However, in these optical experiments, entanglement was swapped conditional on the occurrence of preset photon coincidence events. These events were detected only in a small fraction of experimental runs due to the photon loss on optical components, lack of logic operations to completely distinguish all four Bell states, and restriction of photon detectors' efficiency [17]. Experiments have realized heralded entanglement between two spatially separated atomic qubits, each entangled with its emitted photons before a partial Bell state analysis on these photons [18,19]; the

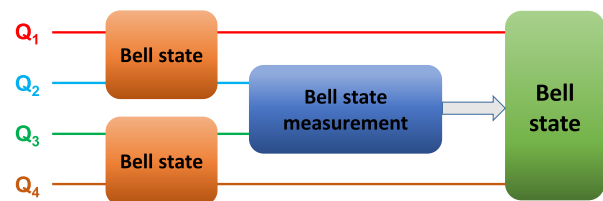


FIG. 1. Sketch of entanglement swapping. Initially,  $Q_1$  is entangled with  $Q_2$  in a Bell state, and  $Q_3$  with  $Q_4$ , but there is no correlation between  $Q_1$  and  $Q_4$ . A joint measurement on  $Q_2$  and  $Q_3$  in the Bell basis will project  $Q_1$  and  $Q_4$  to one of four possible Bell states depending on the outcome of the  $Q_2$ - $Q_3$  measurement.

entanglement was swapped also with a small probability. With photonic continuous variables, unconditional entanglement swapping has been reported [20,21], but where only a small portion of entanglement was preserved after swapping due to the limitation of the degree of entanglement carried by the original entangled beams, which is the main source of the infidelity for teleportation of a continuous-variable state [22]. Although unconditional teleportation has been demonstrated with different kinds of matter qubits, including nuclear magnetic resonance [23], trapped ions [24,25], and superconducting qubits [26,27], where the teleported states were preset and known to the experimenters, deterministic, high-fidelity entanglement swapping has only been realized in an ion trap [28]. As pointed out in Ref. [10], entanglement swapping is the only known procedure that demonstrates the quantum nature of teleportation—the qubit whose state is to be teleported is entangled with another qubit, rendering it impossible to know this state. When realized in a delayed-choice manner [29], this process reveals a more striking feature, that is, one can *a posteriori* determine two already detected particles previously behaved as an entangled pair or as a separable pair.

We here implement a deterministic entanglement swapping experiment with superconducting qubits (labeled from  $Q_1$  to  $Q_4$ ). Our results show that  $Q_1$  and  $Q_4$ , although never coupled to each other, are highly entangled after the swapping process, with the measured concurrence above 0.75. Unlike previous experiments with photonic qubits, the Bell states are produced deterministically and the measurement is single shot, so that the entanglement is swapped unconditionally. We note that an entanglement swapping experiment also with superconducting qubits was briefly mentioned in a recent review [30], but no experimental details have been released up to now. We further realize a delayed-choice entanglement swapping experiment [29], where we choose to perform a Bell state measurement or a separable-state measurement on  $Q_2$  and  $Q_3$  after  $Q_1$  and  $Q_4$  have been detected. The results demonstrate this later choice decides the previous behavior of  $Q_1$  and  $Q_4$ —whether they were entangled or separable. This implies that entanglement is not a reality, but is a manifestation of the statistical correlation of the measured data; the same set of data may show different types of correlations and have different interpretations when grouped in different manners.

The device used to perform the experiment swapping is identical to that used in Ref. [31], where a resonator with a fixed frequency  $\omega_r/2\pi = 5.588$  GHz is controllably coupled to five superconducting Xmon qubits, whose frequencies can be individually adjusted on nanosecond timescales using flux bias lines. The device is sketched in Fig. 2(a), and the optical image shown in Fig. 2(b). Throughout the experiment,  $Q_5$  (unused) is tuned far off resonance with the resonator and the other qubits, and will

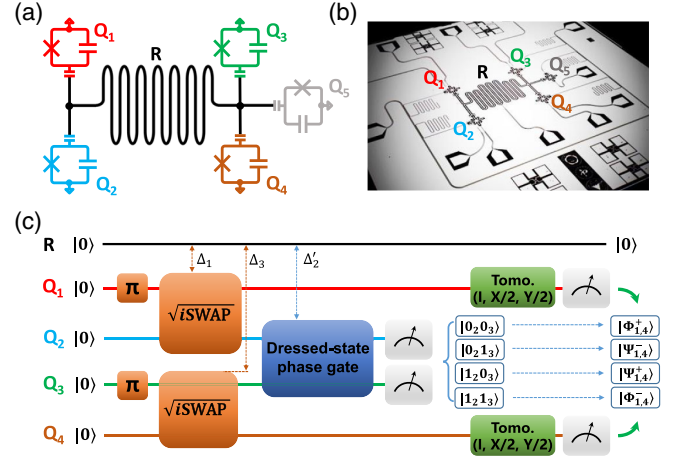


FIG. 2. Device schematic and pulse sequence. (a) Device schematic. Five superconducting Xmon qubits (labeled from  $Q_1$  to  $Q_5$ ) are capacitively coupled to a bus resonator  $R$ . The frequency of each qubit can be adjusted quickly, enabling the relevant qubit-resonator interaction as well as the resonator-induced qubit-qubit couplings to be effectively switched on and off. (b) Optical image of the device. (c) Experimental sequence. The procedure consists of three parts: Generation of Bell states for qubit pairs  $Q_1$ - $Q_2$  and  $Q_3$ - $Q_4$  via resonator-mediated  $\sqrt{i}$ SWAP gates following  $\pi$  pulses applied to  $Q_1$  and  $Q_3$ ; complete Bell state measurement on  $Q_2$  and  $Q_3$ , achieved by sequentially applying a dressed-state phase gate on  $Q_2$  and  $Q_3$  and performing a joint detection in the basis  $\{|0_2\rangle|0_3\rangle, |0_2\rangle|1_3\rangle, |1_2\rangle|0_3\rangle, |1_2\rangle|1_3\rangle\}$ ; 2-qubit quantum state tomography for  $Q_1$  and  $Q_4$ . The detailed pulse sequence is shown in Fig. S3(a) of the Supplemental Material [32].

not be included in the description of the system. The parameters of the system are detailed in the Supplemental Material [32]. All the qubits and the resonator are initially in their ground states. The experiment starts with applying  $\pi$  pulses to  $Q_1$  and  $Q_3$ , transforming each of them from the ground state  $|0\rangle$  to the excited state  $|1\rangle$  at its idle frequency, with the experimental sequence shown in Fig. 2(c). Then the qubit pairs  $Q_1$ - $Q_2$  and  $Q_3$ - $Q_4$  are red detuned from the resonator by  $\Delta_1 = \Delta_2 = 2\pi \times 308$  MHz and  $\Delta_3 = \Delta_4 = 2\pi \times 238$  MHz, respectively. With this setting, the resonator will not exchange photons with the qubits and remain in the ground state, but it can simultaneously mediate two entangling gates, each operating on one qubit pair [35–39], with the coupling between these two qubit pairs being negligible owing to their large detuning [39].

The qubit pair,  $Q_j$ - $Q_k$  ( $j = 1, k = 2$  or  $j = 3, k = 4$ ), evolves to the Bell state  $|\Psi_{j,k}^+\rangle = (|1_j\rangle|0_k\rangle + i|0_j\rangle|1_k\rangle)/\sqrt{2}$  after the corresponding  $\sqrt{i}$ SWAP gate. As soon as  $|\Psi_{j,k}^+\rangle$  is generated,  $Q_j$  and  $Q_k$  are detuned from each other to stop their coupling. The measured density matrices for these two produced entangled pairs are displayed in the Supplemental Material [32]. Their fidelities to the ideal Bell states are, respectively,  $F_{1,2} = 0.982 \pm 0.006$  and  $F_{3,4} = 0.978 \pm 0.007$ .

The product of the two Bell states  $|\Psi_{1,2}^+\rangle$  and  $|\Psi_{3,4}^+\rangle$  can be expanded as

$$|\psi\rangle = \frac{1}{2}[-i|\Psi_{2,3}^+\rangle|\Psi_{1,4}^-\rangle + i|\Psi_{2,3}^-\rangle|\Psi_{1,4}^+\rangle + |\Phi_{2,3}^+\rangle|\Phi_{1,4}^+\rangle - |\Phi_{2,3}^-\rangle|\Phi_{1,4}^-\rangle], \quad (1)$$

where  $|\Psi_{j,k}^\pm\rangle = (|1_j\rangle|0_k\rangle \pm i|0_j\rangle|1_k\rangle)/\sqrt{2}$  and  $|\Phi_{j,k}^\pm\rangle = (|1_j\rangle|1_k\rangle \pm i|0_j\rangle|0_k\rangle)/\sqrt{2}$ . To realize entanglement swapping, we perform a measurement on  $Q_2$  and  $Q_3$  in the Bell basis  $\{|\Psi_{2,3}^+\rangle, |\Psi_{2,3}^-\rangle, |\Phi_{2,3}^+\rangle, |\Phi_{2,3}^-\rangle\}$ , which will project  $Q_1$  and  $Q_4$  to one Bell state. A complete Bell state measurement can be implemented by mapping the Bell basis onto the computational basis  $\{|0_2\rangle|0_3\rangle, |0_2\rangle|1_3\rangle, |1_2\rangle|0_3\rangle, |1_2\rangle|1_3\rangle\}$  through a dressed-state phase gate [40,41]. We note that the  $\sqrt{i}$ SWAP gate only transforms two out of the four Bell states into product states, and thus cannot be used for deterministically distinguishing all the Bell states. To implement the dressed-state phase gate between  $Q_2$  and  $Q_3$ , we tune  $Q_1$  and  $Q_4$  back to their idle frequencies, so that neither of them can interact with other qubits, and then red detune  $Q_2$  and  $Q_3$  from the resonator by the same amount  $\Delta'_2 = \Delta'_3 = 2\pi \times 308$  MHz, switching on their interaction via the resonator-induced virtual photon exchange, with the coupling strength  $\lambda_{2,3} = 2\pi \times 1.14$  MHz. At the same time, we apply a resonant continuous drive to each of these two qubits, whose phase is inverted in the middle of the two-qubit interaction with a duration  $\tau_{2,3} = \pi/2\lambda_{2,3}$ . When the difference of the Rabi frequencies of these two drives is much larger than  $\lambda_{2,3}$ , a dressed-state phase gate between  $Q_2$  and  $Q_3$  is achieved. As a result, the four Bell states of  $Q_2$  and  $Q_3$  evolve as (see Supplemental Material [32])

$$\begin{aligned} |\Psi_{2,3}^+\rangle &\rightarrow i|0_2\rangle|1_3\rangle, & |\Psi_{2,3}^-\rangle &\rightarrow |1_2\rangle|0_3\rangle, \\ |\Phi_{2,3}^+\rangle &\rightarrow i|0_2\rangle|0_3\rangle, & |\Phi_{2,3}^-\rangle &\rightarrow |1_2\rangle|1_3\rangle. \end{aligned} \quad (2)$$

The combination of this transformation and the subsequent detection of  $Q_2$  and  $Q_3$  in the computational basis  $\{|0_2\rangle|0_3\rangle, |0_2\rangle|1_3\rangle, |1_2\rangle|0_3\rangle, |1_2\rangle|1_3\rangle\}$  effectively realizes the complete Bell state analysis, enabling us to distinguish all the four Bell states. Consequently,  $Q_1$  and  $Q_4$  are randomly projected onto one of the four Bell states  $\{|\Phi_{1,4}^+\rangle, |\Psi_{1,4}^-\rangle, |\Psi_{1,4}^+\rangle, |\Phi_{1,4}^-\rangle\}$  depending on the  $Q_2$ - $Q_3$  measurement outcome. During the  $Q_2$ - $Q_3$  Bell-state measurement,  $Q_1$  and  $Q_4$  respectively stay at their idle frequencies, so that the interactions of each of them with the resonator and with any other qubit are effectively switched off due to the large detunings.

After the Bell state analysis, we perform joint 2-qubit state tomography to reconstruct the density matrix for  $Q_1$  and  $Q_4$ . The measured density matrices of  $Q_1$  and  $Q_4$  conditional on the measurement outcomes  $|0_2\rangle|0_3\rangle$ ,

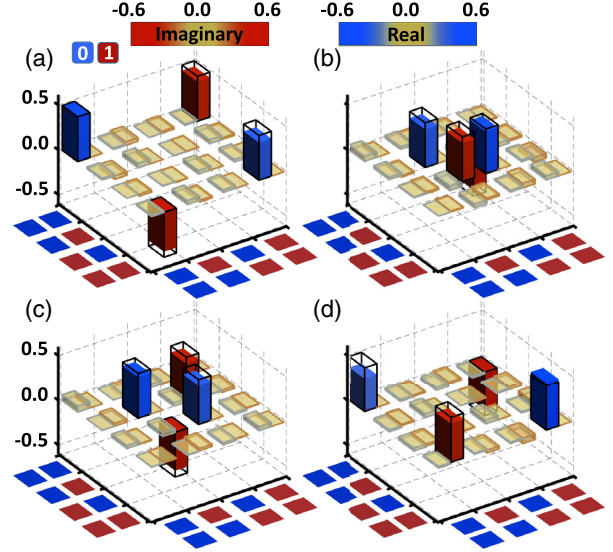


FIG. 3. Measured  $Q_1$ - $Q_4$  density matrices conditional on the four  $Q_2$ - $Q_3$  measurement outcomes: (a)  $|0_2\rangle|0_3\rangle$ ; (b)  $|0_2\rangle|1_3\rangle$ ; (c)  $|1_2\rangle|0_3\rangle$ ; (d)  $|1_2\rangle|1_3\rangle$ . The results are obtained with the experiment sequence shown in Fig. 2(c). Each matrix element is characterized by two color bars, one for the real part and the other for the imaginary part. The black wire frames denote the matrix elements of the ideal output states.

$|0_2\rangle|1_3\rangle$ ,  $|1_2\rangle|0_3\rangle$ , and  $|1_2\rangle|1_3\rangle$  of  $Q_2$  and  $Q_3$  are displayed in Figs. 3(a)–3(d), respectively. The readout error of each qubit is corrected when reconstructing these density matrices. Ideally, for these four outcomes  $Q_1$  and  $Q_4$  are projected onto  $|\Phi_{1,4}^+\rangle$ ,  $|\Psi_{1,4}^-\rangle$ ,  $|\Psi_{1,4}^+\rangle$ , and  $|\Phi_{1,4}^-\rangle$ , respectively. The fidelities for the four obtained Bell states to the ideal ones are  $F_{\Phi^+} = 0.893 \pm 0.010$ ,  $F_{\Psi^-} = 0.879 \pm 0.010$ ,  $F_{\Psi^+} = 0.872 \pm 0.011$ , and  $F_{\Phi^-} = 0.884 \pm 0.010$ , with the concurrences  $C_{\Phi^+} = 0.794 \pm 0.020$ ,  $C_{\Psi^-} = 0.779 \pm 0.020$ ,  $C_{\Psi^+} = 0.758 \pm 0.024$ , and  $C_{\Phi^-} = 0.785 \pm 0.021$ , respectively. These results show that  $Q_4$  ( $Q_1$ ) inherits most of the entanglement of  $Q_2$  with  $Q_1$  ( $Q_3$  with  $Q_4$ ) after the swapping, which is in stark contrast with experiments with photonic continuous variables [20,21], where only a small portion of entanglement is inherited (e.g., about 29% in Ref. [20]). As the readout error of each qubit is corrected when reconstructing the  $Q_1$ - $Q_4$  output density matrices, the infidelities mainly come from imperfect preparation of the  $Q_1$ - $Q_2$  and  $Q_3$ - $Q_4$  Bell states, imperfection of the  $Q_2$ - $Q_3$  dressed-state phase gate, and decoherence effects of  $Q_1$  and  $Q_4$  during this gate.

We note that the deterministic entanglement swapping requires reliable Bell state measurement on  $Q_2$  and  $Q_3$ , whose performance depends on the quality of the dressed-state phase gate and the single-shot state readout fidelities of  $Q_2$  and  $Q_3$ . The fidelity of the dressed-state phase gate is  $F_{gt} \approx 0.966$ , while the average readout fidelities of  $Q_2$  and  $Q_3$  are  $F_2 = 0.95$  and  $F_3 = 0.94$ , where  $F_j = (F_{0,j} + F_{1,j})/2$ , with  $F_{0,j}$  and  $F_{1,j}$  denoting

the  $|0\rangle$ - and  $|1\rangle$ -state readout fidelities of  $Q_j$ , whose values are listed in Table S1 of the Supplemental Material [32]. Without readout error corrections, the average measurement fidelity of the four Bell states is roughly  $F_{\phi^+}F_{\psi^-}F_{\psi^+}F_{\phi^-} \approx 0.863$ , and each of the four corresponding  $Q_1$ - $Q_4$  output states, as shown in Fig. S4 of the Supplemental Material [32], has a fidelity above 0.76 and a concurrence exceeding 0.54.

Going one step further, we delay the  $Q_2$ - $Q_3$  Bell state measurement until the joint  $Q_1$ - $Q_4$  state has been detected. The detailed pulse sequence is shown in Fig. S3(b) of the Supplemental Material [32], where the  $Q_2$ - $Q_3$  readout pulse is applied about 219 ns after the end of  $Q_1$ - $Q_4$  readout pulse. Since the correlation between the outcomes of  $Q_2$ - $Q_3$  measurement and  $Q_1$ - $Q_4$  measurement is independent of their temporal order, this arrangement will result in entanglement swapping in a delayed manner [29]. According to  $Q_2$ - $Q_3$  Bell state measurement outcomes, the data of  $Q_1$ - $Q_4$  joint state measurement are sorted into four subsets, from which four density matrices are reconstructed, and shown in Figs. 4(a)–4(d). As in the non-delayed case, these four density matrices correspond to four Bell states, with the respective fidelities  $F_{\phi^+} = 0.891 \pm 0.012$ ,  $F_{\psi^-} = 0.891 \pm 0.012$ ,  $F_{\psi^+} = 0.896 \pm 0.010$ , and  $F_{\phi^-} = 0.897 \pm 0.010$ , and concurrences  $C_{\phi^+} = 0.815 \pm 0.026$ ,  $C_{\psi^-} = 0.816 \pm 0.024$ ,  $C_{\psi^+} = 0.806 \pm 0.022$ , and  $C_{\phi^-} = 0.807 \pm 0.019$ . The fidelities and concurrences are slightly higher than those in the nondelayed case due to the fact that  $Q_1$ - $Q_4$  joint state is detected earlier so that the measured data are less affected by decoherence effects.

We also perform another experiment, where we choose to measure  $Q_2$  and  $Q_3$  in the computational basis (without

performing the dressed-state phase gate before detection of their states). Again, this measurement is performed after  $Q_1$ - $Q_4$  joint state detection, with the pulse sequence shown in Fig. S3(c) of the Supplemental Material [32]. The density matrices reconstructed from the four subsets of  $Q_1$ - $Q_4$  measurement data, each associated with one of  $Q_2$ - $Q_3$  measurement outcomes  $\{|0_2\rangle|0_3\rangle, |0_2\rangle|1_3\rangle, |1_2\rangle|0_3\rangle, |1_2\rangle|1_3\rangle\}$ , are presented in Figs. 4(e)–4(h), respectively. As expected, these matrices correspond to product states  $\{|1_1\rangle|1_4\rangle, |1_1\rangle|0_4\rangle, |0_1\rangle|1_4\rangle, |0_1\rangle|0_4\rangle\}$  with the fidelities  $\{0.907 \pm 0.011, 0.914 \pm 0.009, 0.930 \pm 0.009, 0.949 \pm 0.008\}$ . The concurrence associated with each of these reconstructed matrices is approximate to 0 (see Table S4 of the Supplemental Material [32]).

The above results demonstrate whether or not the already measured qubits  $Q_1$  and  $Q_4$  previously behaved as an entangled pair depends on the later choice of the type of measurement on  $Q_2$  and  $Q_3$ . As a generalization of Wheeler's delayed-choice experiment proposed for illustrating the wave-particle duality of a single particle [42], the delayed-choice entanglement swapping experiment reveals the entanglement-separability duality of two particles [43]. A realization of this gedanken experiment was previously reported with photonic qubits [17], but where only two out of four basis states could be distinguished in each of the two mutually exclusive measurements, so that the entanglement-separability duality was only partially demonstrated: Whether the  $Q_1$ - $Q_4$  states associated with the two indistinguishable  $Q_2$ - $Q_3$  basis states manifested a quantum or a classical correlation could not be confirmed. Another problem is only a small fraction of events coinciding with the distinguishable basis states was detected owing to the

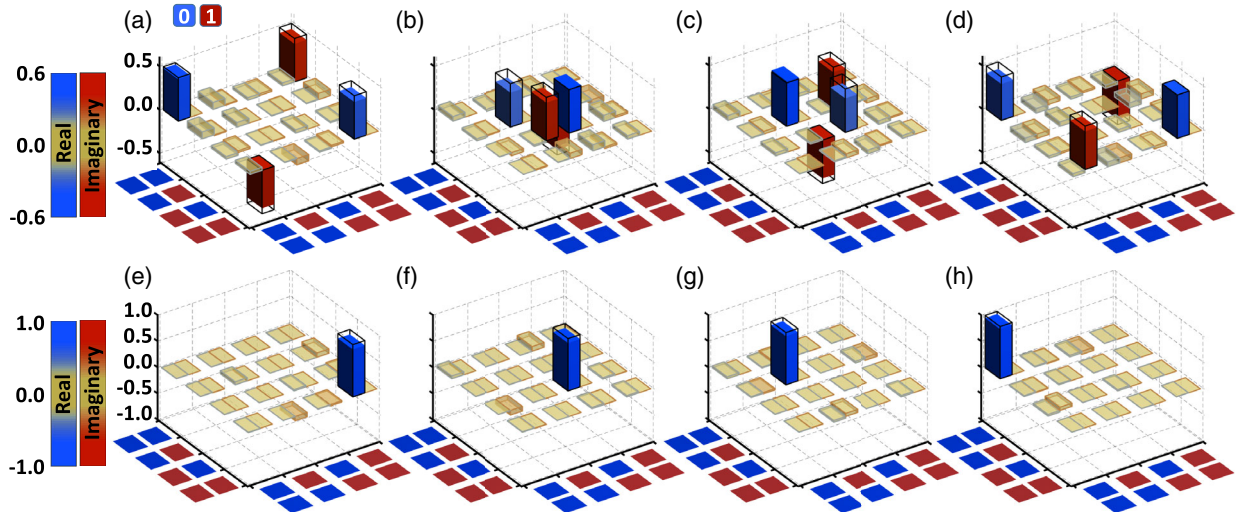


FIG. 4. Measured  $Q_1$ - $Q_4$  density matrices conditional on outcomes of delayed-choice  $Q_2$ - $Q_3$  measurement. (a)–(d) Results obtained from the four subsets of data correlated with the outcomes  $\{|0_2\rangle|0_3\rangle, |0_2\rangle|1_3\rangle, |1_2\rangle|0_3\rangle, |1_2\rangle|1_3\rangle\}$  of  $Q_2$ - $Q_3$  measurement performed after the dressed-state phase gate. Compared with Fig. 2(c), the temporal orders of  $Q_2$ - $Q_3$  Bell measurement and  $Q_1$ - $Q_4$  joint state tomography are inverted, with the experimental pulse sequence shown in the Supplemental Material [32]. (e)–(h) Results obtained from the four subsets of data correlated with the outcomes of the later  $Q_2$ - $Q_3$  measurement without the dressed-state phase gate.

photon loss on optical components (only 4.4% photons left) and nonunity photon detection efficiency.

We have demonstrated deterministic entanglement swapping with superconducting qubits controllably coupled to a resonator. The qubit-qubit couplings mediated by the resonator allows for both the controlled generation of the Bell states and complete Bell state analysis. We have further deterministically realized delayed-choice entanglement swapping, demonstrating whether two qubits exhibited entangled or separable behavior can be *a posteriori* decided after they have been measured. Our results indicate quantum entanglement of two quantum systems is a manifestation of the statistical correlations of the measured data, instead of a reality.

We thank Haohua Wang at Zhejiang University for technical support. This work was supported by the National Natural Science Foundation of China (Grants No. 11674060, No. 11874114, and No. 11875108), and the Strategic Priority Research Program of Chinese Academy of Sciences (Grant No. XDB28000000).

\*zbyang@fzu.edu.cn

†kaixu@iphy.ac.cn

\*t96034@fzu.edu.cn

- [1] A. Einstein, B. Podolsky, and N. Rosen, *Phys. Rev.* **47**, 777 (1935).
- [2] J. S. Bell, *Physics* **1**, 195 (1964).
- [3] J. F. Clauser, M. A. Horne, A. Shimony, and R. A. Holt, *Phys. Rev. Lett.* **23**, 880 (1969).
- [4] C. H. Bennett, G. Brassard, C. Crépeau, R. Jozsa, A. Peres, and W. K. Wootters, *Phys. Rev. Lett.* **70**, 1895 (1993).
- [5] R. Raussendorf and H. J. Briegel, *Phys. Rev. Lett.* **86**, 5188 (2001).
- [6] M. Żukowski, A. Zeilinger, M. A. Horne, and A. K. Ekert, *Phys. Rev. Lett.* **71**, 4287 (1993).
- [7] W. Dür, H.-J. Briegel, J. I. Cirac, and P. Zoller, *Phys. Rev. A* **59**, 169 (1999).
- [8] S. Bose, V. Vedral, and P. L. Knight, *Phys. Rev. A* **57**, 822 (1998).
- [9] J.-W. Pan, D. Bouwmeester, H. Weinfurter, and A. Zeilinger, *Phys. Rev. Lett.* **80**, 3891 (1998).
- [10] J.-W. Pan, M. Daniell, S. Gasparoni, G. Weihs, and A. Zeilinger, *Phys. Rev. Lett.* **86**, 4435 (2001).
- [11] H. de Riedmatten, I. Marcikic, J. A. W. van Houwelingen, W. Tittel, H. Zbinden, and N. Gisin, *Phys. Rev. A* **71**, 050302(R) (2005).
- [12] M. Halder, A. Beveratos, N. Gisin, V. Scarani, C. Simon, and H. Zbinden, *Nat. Phys.* **3**, 692 (2007).
- [13] C.-Y. Lu, T. Yang, and J.-W. Pan, *Phys. Rev. Lett.* **103**, 020501 (2009).
- [14] C. Schmid, N. Kiesel, U. K. Weber, R. Ursin, A. Zeilinger, and H. Weinfurter, *New J. Phys.* **11**, 033008 (2009).
- [15] F. Sciarrino, E. Lombardi, G. Milani, and F. De Martini, *Phys. Rev. A* **66**, 024309 (2002).
- [16] T. Jennewein, G. Weihs, J.-W. Pan, and A. Zeilinger, *Phys. Rev. Lett.* **88**, 017903 (2001).
- [17] X.-S. Ma, S. Zotter, J. Kofler, R. Ursin, T. Jennewein, Č. Brukner, and A. Zeilinger, *Nat. Phys.* **8**, 479 (2012).
- [18] D. N. Matsukevich, P. Maunz, D. L. Moehring, S. Olmschenk, and C. Monroe, *Phys. Rev. Lett.* **100**, 150404 (2008).
- [19] Z.-S. Yuan, Y.-A. Chen, B. Zhao, S. Chen, J. Schmiedmayer, and J.-W. Pan, *Nature (London)* **454**, 1098 (2008).
- [20] X. Jia, X. Su, Q. Pan, J. Gao, C. Xie, and K. Peng, *Phys. Rev. Lett.* **93**, 250503 (2004).
- [21] N. Takei, H. Yonezawa, T. Aoki, and A. Furusawa, *Phys. Rev. Lett.* **94**, 220502 (2005).
- [22] S. L. Braunstein and H. J. Kimble, *Phys. Rev. Lett.* **80**, 869 (1998).
- [23] M. A. Nielsen, E. Knill, and R. Laflamme, *Nature (London)* **396**, 52 (1998).
- [24] M. Riebe, H. Häffner, C. F. Roos, W. Hänsel, J. Benhelm, G. P. T. Lancaster, T. W. Körber, C. Becher, F. Schmidt-Kaler, D. F. V. James, and R. Blatt, *Nature (London)* **429**, 734 (2004).
- [25] M. D. Barrett, J. Chiaverini, T. Schaetz, J. Britton, W. M. Itano, J. D. Jost, E. Knill, C. Langer, D. Leibfried, R. Ozeri, and D. J. Wineland, *Nature (London)* **429**, 737 (2004).
- [26] M. Baur, A. Fedorov, L. Steffen, S. Filipp, M. P. da Silva, and A. Wallraff, *Phys. Rev. Lett.* **108**, 040502 (2012).
- [27] L. Steffen, A. Fedorov, M. Oppliger, Y. Salathe, P. Kurpiers, M. Baur, G. Puebla-Hellmann, C. Eichler, and A. Wallraff, *Nature (London)* **500**, 319 (2013).
- [28] M. Riebe, T. Monz, K. Kim, A. S. Villar, P. Schindler, M. Chwalla, M. Hennrich, and R. Blatt, *Nat. Phys.* **4**, 839 (2008).
- [29] A. Peres, *J. Mod. Opt.* **47**, 139 (2000).
- [30] G. Wendin, *Rep. Prog. Phys.* **80**, 106001 (2017).
- [31] C. Song, S.-B. Zheng, P. Zhang, K. Xu, L. Zhang, Q. Guo, W. Liu, D. Xu, H. Deng, K. Huang, D. Zheng, X. Zhu, and H. Wang, *Nat. Commun.* **8**, 1061 (2017).
- [32] See Supplemental Material at <http://link.aps.org/supplemental/10.1103/PhysRevLett.123.060502>, which includes Refs. [33,34] for the device parameters, characterization of the Bell states produced by  $\sqrt{i}$ SWAP gates, realization of complete Bell state measurement, detailed experimental pulse sequences, results without readout error corrections for Bell state measurement, numerical simulations, experimental setup, and details on qubits' readout.
- [33] K. Xu, J.-J. Chen, Y. Zeng, Y.-R. Zhang, C. Song, W. Liu, Q. Guo, P. Zhang, D. Xu, H. Deng, K. Huang, H. Wang, X. Zhu, D. Zheng, and H. Fan, *Phys. Rev. Lett.* **120**, 050507 (2018).
- [34] D. Sank, Ph.D. thesis, University of California, Santa Barbara, 2014.
- [35] S.-B. Zheng and G.-C. Guo, *Phys. Rev. Lett.* **85**, 2392 (2000).
- [36] S. Osnaghi, P. Bertet, A. Auffeves, P. Maioli, M. Brune, J. M. Raimond, and S. Haroche, *Phys. Rev. Lett.* **87**, 037902 (2001).
- [37] J. Majer, J. M. Chow, J. M. Gambetta, Jens Koch, B. R. Johnson, J. A. Schreier, L. Frunzio, D. I. Schuster, A. A. Houck, A. Wallraff, A. Blais, M. H. Devoret, S. M. Girvin, and R. J. Schoelkopf, *Nature (London)* **449**, 443 (2007).

- [38] Y.-P. Zhong, D. Xu, P. Wang, C. Song, Q.-J. Guo, W.-X. Liu, K. Xu, B.-X. Xia, C.-Y. Lu, S. Han, J.-W. Pan, and H. Wang, *Phys. Rev. Lett.* **117**, 110501 (2016).
- [39] C. Song, K. Xu, W. Liu, C.-P. Yang, S.-B. Zheng, H. Deng, Q. Xie, K. Huang, Q. Guo, L. Zhang, P. Zhang, D. Xu, D. Zheng, X. Zhu, H. Wang, Y.-A. Chen, C.-Y. Lu, S. Han, and J.-W. Pan, *Phys. Rev. Lett.* **119**, 180511 (2017).
- [40] Q. Guo, S.-B. Zheng, J. Wang, C. Song, P. Zhang, K. Li, W. Liu, H. Deng, K. Huang, D. Zheng, X. Zhu, H. Wang, C.-Y. Lu, and J.-W. Pan, *Phys. Rev. Lett.* **121**, 130501 (2018).
- [41] C. Song, D. Xu, P. Zhang, J. Wang, Q. Guo, W. Liu, K. Xu, H. Deng, K. Huang, D. Zheng, S.-B. Zheng, H. Wang, X. Zhu, C.-Y. Lu, and J.-W. Pan, *Phys. Rev. Lett.* **121**, 030502 (2018).
- [42] J. A. Wheeler, in *Quantum Theory and Measurement*, edited by J. A. Wheeler and W. H. Zurek (Princeton University Press, Princeton, NJ, 1984), p. 182.
- [43] Č. Brukner, M. Aspelmeyer, and A. Zeilinger, *Found. Phys.* **35**, 1909 (2005).